



Supplement of

FESOM2.1-REcoM3-MEDUSA2: an ocean–sea ice–biogeochemistry model coupled to a sediment model

Ying Ye et al.

Correspondence to: Ying Ye (ying.ye@awi.de)

The copyright of individual parts of the supplement might differ from the article licence.

MEDUSA Setup and Selected Configuration Options

S1 Formulation

S1.1 Early diagenetic reaction network and chemical composition

The reaction network set up in this version of MEDUSA includes the following processes:

- Calcite dissolution;
- Opal dissolution;
- Organic Matter (OM) degradation: three different pathways are considered
 - oxic respiration
 - nitrate reduction
 - sulfate reduction

Mn(IV) and Fe(III) reduction pathways are disregarded here as they play, globally speaking, only negligible roles as TEAs (terminal electron acceptors) in comparison to the three pathways considered with O_2 , NO_3^- and SO_4^{2-} as TEAs, resp. (Thullner et al., 2009).

The adopted model configuration includes CO_2 , HCO_3^- , CO_3^{2-} , O_2 , NO_3^- and NH_4^+ as solutes, and two classes of organic matter (a fast and a slowly metabolizable one), clay and calcite as solids. For simplicity, the ΣNH_3 and ΣH_2S systems are reduced to NH_4^+ and HS^- , resp.

S1.2 Boundary conditions

Temperature, pressure and salinity for each sediment column are those of the bottom ocean cell that it is in contact with and similarly for the solutes' concentrations at the sediment–water–interface (SWI). The boundary conditions for NH_4^+ , HS^- and SO_4^{2-} , which are not among the tracers considered in REcoM3p, the REcoM3 variant used here, are set as follows: the concentrations of NH_4^+ and HS^- at the SWI is set to 0 (Jourabchi et al., 2008; Thullner et al., 2009) and that of SO_4^{2-} is derived from the sulfate–salinity relationship, i.e. $[SO_4^{2-}]_{SWI} / [mol (kg-SW)^{-1}] = (0.14/96.062) \times (S/1.80655)$ (Dickson et al., 2007, chap. 6, p. 10), where S is the salinity at the SWI.

For solids, a flux-continuity condition is adopted at the SWI: solid material deposited at the sea-floor gets transferred to the sediment across the SWI.

The organic matter REcoM3p has a C : N(: P) composition that varies in space and time. C : N : P compositions of organic matter classes in MEDUSA may, must, however, remain constant in time; they may only be spatially variable. Organic matter reaching the sea-floor is therefore handled as if it was a mixture of two end-member classes, each one with a fixed C : N : P ratio: one with C : N = 106 : 21 : 1.3125 (fast metabolizable), and one with C : N : P = 200 : 11 : 0.6875 (slowly metabolizable). Since REcoM3p does not consider P, the N : P ratio of the two end-member classes in MEDUSA is assumed to be at the Redfield ratio of 16:1.

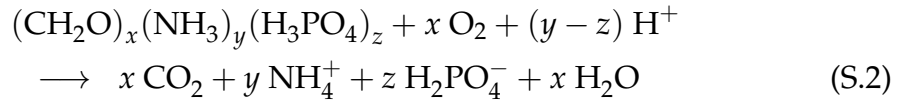
S1.3 Model reactions

The equations used to represent the chemical reactions that describe the processes considered are as follows:

R^1 — CaCO₃ dissolution:

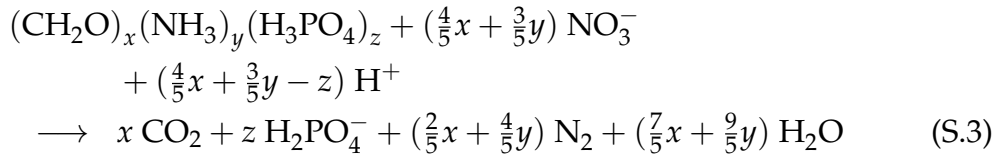


R^2 & R^3 – oxidation of ‘fast’ and ‘slow’ OM classes, resp., by oxic respiration:

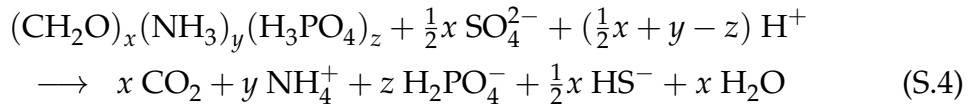


where $x = 106$, $y = 21$ and $z = 1.3125$ for the ‘fast,’ and $x = 200$, $y = 11$ and $z = 0.6875$ for the ‘slow’ OM class

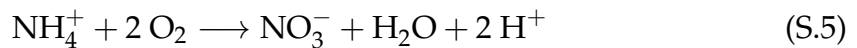
R^4 & R^5 – oxidation of ‘fast’ and ‘slow’ OM classes, resp., by nitrate reduction and full denitrification:



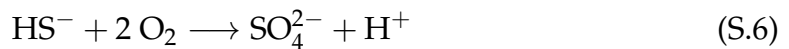
R^6 & R^7 – oxidation of ‘fast’ and ‘slow’ OM classes, resp., by sulfate reduction:



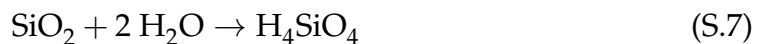
R^8 – ammonium re-oxidation by O₂:



R^9 – sulfide re-oxidation by O₂:



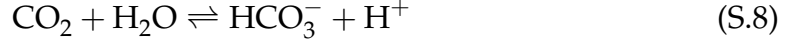
R^{10} – opal dissolution:



S1.4 Equilibria

As a consequence of the simplifications adopted for the ammonium and hydrogen sulfide (hydrosulfuric acid) systems, only the carbonate system equilibria need to be considered:

E^1 (first dissociation of carbonic acid):



E^2 (second dissociation of carbonic acid):



S2 Unified Formulation

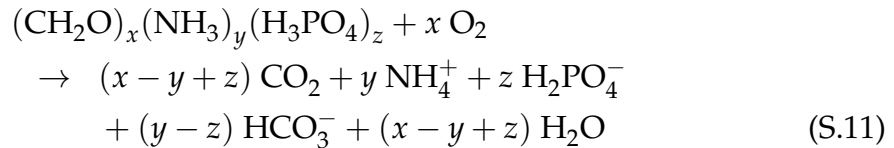
The equations from the previous section are modified in order to discard the H^+ ion, by introduction of the $\text{CO}_2\text{--HCO}_3^-$ equilibrium $\text{CO}_2 + \text{H}_2\text{O} \rightleftharpoons \text{HCO}_3^- + \text{H}^+$. Accordingly, if one side of chemical reaction includes a term $n \text{H}^+$, that term is substituted with $n \text{CO}_2 + n \text{H}_2\text{O}$, and a term $n \text{HCO}_3^-$ is added to the other side. Finally, the two equilibria E^1 and E^2 are furthermore lumped into one (E^{1+2}).

This same procedure was also adopted by Wang and Van Cappellen (1996) and Thullner et al. (2009).

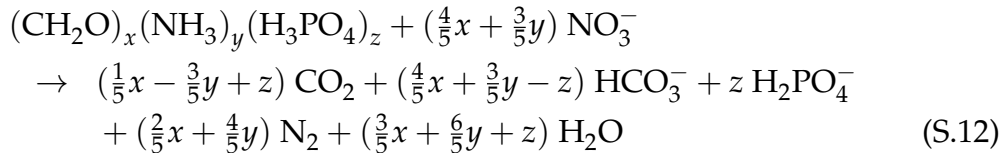
R^1 (CaCO_3 dissolution):



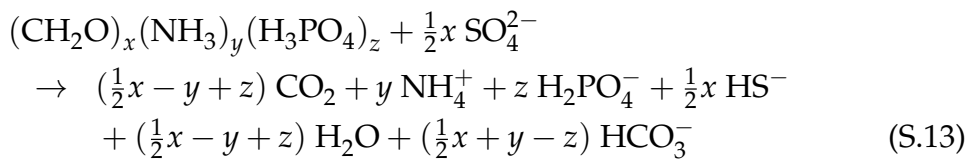
R^2 & R^3 (oxic respiration):



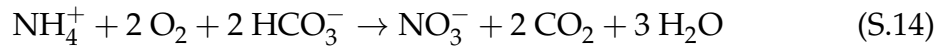
R^4 & R^5 (nitrate reduction):



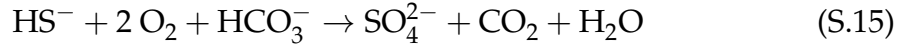
R^6 & R^7 (sulfate reduction):



R^8 (ammonium re-oxidation):



R^9 (sulfide re-oxidation):



R^{10} (opal dissolution):



S2.1 Equilibrium

E^{1+2} (carbonate system equilibrium):



S3 Kinetic Rate Laws and Equilibrium Relationship

Reaction rates are written here as \hat{R} values, i.e., per unit volume of total sediment (solids + porewater): for solids' degradation/dissolution rates, units are each time kg solid (m³ total sediment)⁻¹ yr⁻¹; for reactions between solutes only, the rates are expressed in mol solute (m³ total sediment)⁻¹ yr⁻¹.

S3.1 Calcite dissolution

The classical formulation in $(1 - \Omega)^{4.5}$ (Keir, 1980; Archer, 1991) was adopted:

$$\hat{R}_1 = k_1(1 - \varphi) \cdot [\text{Calc}] \cdot ((1 - [\text{CO}_3^{2-}]/C_{\text{cs}})^{\oplus})^{n_1}$$

where

- $k_1 = 1 \text{ d}^{-1} = 365.25 \text{ yr}^{-1}$ (Archer, 1991);
- $n_1 = 4.5$ (Keir, 1980; Archer, 1991);
- $(\dots)^{\oplus}$ denotes the positive part of (\dots) ;
- C_{cs} is the CO_3^{2-} concentration at saturation with respect to calcite in seawater.

S3.2 OM oxidation by oxic respiration

The rate of oxic respiration (eq. S.11) is proportional to the concentration of organic matter (OM) and to a (hyperbolic) Monod factor in the porewater concentration of O_2 :

$$\hat{R}_{2,3} = k_{f,s}(1 - \varphi) \cdot [OM_{f,s}] \cdot \frac{[O_2]}{C_{\text{hox}} + [O_2]},$$

where

- $k_f = 3.2 \times 10^{-1} \text{ yr}^{-1}$ (for \hat{R}_2);
- $k_s = 3.2 \times 10^{-3} \text{ yr}^{-1}$ (for \hat{R}_3);
- $C_{\text{hox}} = 3 \mu\text{mol L}^{-1}$ (Soetaert et al., 1996) is the half-saturation concentration of O_2 for the oxic remineralisation of organic matter; the same value is used for both fast and slow OM classes.

The values for k_f and k_s were derived by considering typical deep-sea values of $10^{-9} \text{ s}^{-1} \simeq 3.2 \times 10^{-2} \text{ yr}^{-1}$ (e.g., Emerson, 1985; Archer, 1991). The finally adopted values were then derived by adopting a two-order of magnitude difference between the slow and fast metabolizable classes (Soetaert et al., 1996), which led us to adopt a one order of magnitude higher value than the typical one for the fast metabolizable class (i.e., $k_f = 3.2 \times 10^{-1} \text{ yr}^{-1}$) and a one order of magnitude lower value for the slowly metabolizable class (i.e., $k_s = 3.2 \times 10^{-3} \text{ yr}^{-1}$).

S3.3 OM oxidation by nitrate reduction, with full denitrification

The rate of OM degradation by nitrate reduction, and full denitrification (R^4 and R^5 , Eq. S.12), is again proportional to the concentration of OM. It is furthermore proportional to a Monod factor in the porewater concentration of NO_3^- , and to a hyperbolic inhibition factor in the porewater concentration of O_2 :

$$\hat{R}_{4,5} = k_{f,s}(1 - \varphi) \cdot [OM_{f,s}] \cdot \frac{[NO_3^-]}{C_{\text{hnr}} + [NO_3^-]} \cdot \frac{C_{\text{ino}}}{C_{\text{ino}} + [O_2]},$$

where

- k_f and k_s are the same as in \hat{R}_2 and \hat{R}_3 above;
- $C_{\text{hnr}} = 30 \mu\text{mol L}^{-1}$ (Soetaert et al., 1996) is the half-saturation concentration of NO_3^- for organic matter degradation by nitrate reduction and denitrification;
- $C_{\text{ino}} = 10 \mu\text{mol L}^{-1}$ (Soetaert et al., 1996) is the characteristic inhibition concentration of O_2 for the oxidation of organic matter by nitrate reduction.

The same C_{hnr} and C_{ino} are used for slow and fast metabolizable OM.

S3.4 OM oxidation by sulfate reduction

The rate of OM degradation by sulfate reduction (R^6 and R^7 , Eq. S.13) is again proportional to the concentration of OM. It is furthermore proportional to a Monod factor in the porewater concentration of SO_4^{2-} , and to two hyperbolic inhibition factors in the porewater concentrations of NO_3^- and O_2 , resp.:

$$\hat{R}_{6,7} = k_{f,s}(1 - \varphi) \cdot [\text{OM}_{f,s}] \cdot \frac{[\text{SO}_4^{2-}]}{C_{\text{hsr}} + [\text{SO}_4^{2-}]} \cdot \frac{C_{\text{isn}}}{C_{\text{isn}} + [\text{NO}_3^-]} \cdot \frac{C_{\text{iso}}}{C_{\text{iso}} + [\text{O}_2]}$$

with

- k_f and k_s are the same as in \hat{R}_2 and \hat{R}_3 above;
- $C_{\text{hsr}} = 0.5 \text{ mmol L}^{-1}$ is the half-saturation concentration of SO_4^{2-} for organic matter degradation by sulfate reduction, derived from the value of 1 mmol L^{-1} that Jourabchi et al. (2008) adopted in their ramp-law;
- $C_{\text{isn}} = 5 \mu\text{mol L}^{-1}$ (Soetaert et al., 1996) is the characteristic inhibition concentration of NO_3^- for the oxidation of organic matter by sulfate reduction;
- $C_{\text{iso}} = 10 \mu\text{mol L}^{-1}$ (Soetaert et al., 1996) is the characteristic inhibition concentration of O_2 for the oxidation of organic matter by sulfate reduction.

The same C_{hsr} , C_{iso} and C_{isn} are used for slow and fast metabolizable OM.

S3.5 Ammonium re-oxidation by O_2 (nitrification)

The rate of oxidation of NH_4^+ by O_2 (eq. S.14) is first order in both $[\text{NH}_4^+]$ and $[\text{O}_2]$.

$$\hat{R}_8 = k_8 \varphi \cdot [\text{NH}_4^+] \cdot [\text{O}_2]$$

The rate constant k_8 is set to $10^4 (\text{mol/m}^3)^{-1} \text{yr}^{-1}$ (Jourabchi et al., 2008).

S3.6 Sulfide re-oxidation by O_2

Oxidation of HS^- by O_2 (eq. S.15): first order in both $[\text{HS}^-]$ and $[\text{O}_2]$

$$\hat{R}_9 = k_9 \varphi \cdot [\text{HS}^-] \cdot [\text{O}_2]$$

Selecting a value for the rate constant k_9 proved tricky. Previously published models used widely different values*:

- Van Cappellen and Wang (1995) set it to $3 \times 10^8 \text{ M}^{-1} \text{yr}^{-1}$ in the deep sea and to $6 \times 10^8 \text{ M}^{-1} \text{yr}^{-1}$ on the shelves, with reference to Morse et al. (1987);

*In the following, the quoted figures are expressed in the units in which they were reported in the respective references, and 'M' is understood to stand for mol L^{-1} .

- Van Cappellen and Wang (1996) and Wang and Van Cappellen (1996) set it to $1.6 \times 10^5 \text{ M}^{-1} \text{ yr}^{-1}$, with reference to Millero et al. (1987);
- Jourabchi et al. (2008) set it to $3 \times 10^8 \text{ M}^{-1} \text{ yr}^{-1}$, with reference to Van Cappellen and Wang (1995);
- Thullner et al. (2009) set it to $3 \times 10^8 \text{ M}^{-1} \text{ yr}^{-1}$, with reference to Van Cappellen and Wang (1995);
- Arndt et al. (2011) use a different rate law expression:

$$R_{A11} = k_{T_S, O_2} \cdot \frac{O_2}{K_{T_{O_2}, \text{redox}} + O_2} \cdot T_S,$$

with $k_{T_S, O_2} = 6 \text{ yr}^{-1}$ (calibrated) and $K_{T_{O_2}, \text{redox}} = 20 \text{ mmol m}^{-3}$. The coefficients in the two expressions can only be compared for $O_2 \ll K_{T_{O_2}, \text{redox}}$, in which case $k_9 \simeq k_{T_S, O_2} / K_{T_{O_2}, \text{redox}} = 6/20 = 0.3 \text{ (mmol m}^{-3}\text{)}^{-1} \text{ yr}^{-1} = 3 \times 10^5 \text{ M}^{-1} \text{ yr}^{-1}$.

This three orders of magnitude differences between the adopted values seem difficult to reconcile a priori. However, it appears that the rate of sulfide oxidation strongly depends on whether it takes place inorganically or is biologically mediated. In this latter case, it may indeed proceed orders of magnitude faster than in abiotic cases (the presence of Fe^{2+} or Mn^{2+} also appears to promote the reaction, albeit to a lesser extent).

We therefore chose to use $k_9 = 5 \times 10^5 \text{ (mol m}^{-3}\text{)}^{-1} \text{ yr}^{-1}$, a value intermediate between the deep-sea and shelf values of Van Cappellen and Wang (1995), slightly biased towards the shelf end-member, as the reaction is important mainly in shallower waters in our model.

S3.7 Opal dissolution

The opal dissolution rate expression in $(C_{\text{sat}} - C)$ (Boudreau, 1990) is considered. Accordingly, the dissolution rate is taken to be proportional to the opal content itself, and to the difference from the saturation concentration of H_4SiO_4 with respect to opal:

$$\hat{R}_{10} = k_{10}(1 - \varphi) \cdot [\text{Opal}] \cdot (C_{\text{osp}} - [\text{H}_4\text{SiO}_4])^{\oplus}$$

where

- $k_{10} = 0.03 \text{ (mol/m}^3\text{)}^{-1} \text{ yr}^{-1}$;
- C_{osp} is the asymptotic (“saturation”) concentration for opal dissolution, set here to $1000 \mu\text{mol kg-SW}^{-1}$ (Archer et al., 1993, following Hurd, 1973);
- and $(\dots)^{\oplus}$ denotes again the positive part of (\dots) .

S3.8 Carbonate equilibrium

The equilibrium constant for the chemical equilibrium (S.17) is derived from the local sediment-top boundary conditions for $[\text{CO}_2]$, $[\text{HCO}_3^-]$, and $[\text{CO}_3^{2-}]$, (standard procedure in MEDUSA). As a consequence, the equilibrium constant is consistent with the carbonate speciation in the host model (REcoM3p).

S4 Spatial Extent and Discretization Grid

The model sediment columns extend down to 50 cm below the sediment–water interface. The top-most 10 cm are mixed by bioturbation. The mixed-layer part is covered with a node-to-node grid of 21 points; the 40 cm below are also covered by a node-to-node grid with an additional 50 points (total of 71 points). Both sub-grids follow a 50%–50% quadratic–linear distribution (please refer to the *Technical Reference* in the Supplement to Munhoven (2021) for details about how to set grid properties in MEDUSA v.2).

S5 Milieu Characteristics

A static global exponentially decreasing porosity profile is used for all sediment columns:

$$\varphi(z) = \varphi_0 + (\varphi_0 - \varphi_\infty) \exp(-z/\zeta)$$

where

- z is the depth in the sediment below the SWI, located at $z = 0$, and increasing downwards;
- $\varphi_0 = 0.9$ is the porosity at the SWI;
- $\varphi_\infty = 0.7$ is the porosity at great depth;
- $\zeta = 4$ cm is the spatial scale of variation (Soetaert et al., 1996)

Tortuosity, ϑ^2 , is parametrised as a function of porosity using the modified Weissberg relationship from Boudreau (1997, p. 131):

$$\vartheta^2 = 1 - 2.02 \ln \varphi.$$

S6 Transport Parameters

S6.1 Advection

As all the solids are considered with their physical specific volumes, advection is treated in the usual way (i.e., the advection rate profile is at each time step derived

iteratively from the integrated reaction rate profile). Please refer to Munhoven (2021) for details about how this is done.

S6.1 Bioturbation

Bioturbation is represented as a diffusive process (biodiffusion). The bioturbation coefficient D_b is uniformly set to $0.150 \text{ cm}^2/\text{yr}$, a typical deep-sea value (Emerson, 1985).

S7 Closing the Global Material Balances

S7.1 Loopback fluxes

In order to conserve the total amounts of carbon and other nutrients, as well as alkalinity in the combined ocean–sediment system, solids that leave the model sediment through its lower boundary (at 50 cm depth below the SWI) are formally remineralized and the resulting amounts of carbon, nutrients and alkalinity returned to the surface, mimicking riverine input to the ocean.

S7.2 Compensating for nutrient sinks and alkalinity sources during anoxic OM degradation

The sediment takes up SO_4^{2-} for the oxidation of OM by sulfate reduction. Part of the HS^- produced during OM oxidation by sulfate reduction is re-oxidized to SO_4^{2-} in the oxygenated part of the sediment, but part is not and diffuses back to the overlying bottom seawater. Please notice that, although the boundary conditions at the SWI set the HS^- concentration to 0, this does not imply that the diffusive return flux to the ocean is 0 as well. This latter indeed depends on the sediment–side HS^- concentration gradient, which is not necessarily 0. Although imbalances in the sulfate content of the ocean would be without consequences, the conversion of SO_4^{2-} to HS^- has a non-negligible effect on the alkalinity balance of the ocean, as HS^- carries alkalinity, while SO_4^{2-} does not. Similarly, the alkalinity balance of the ocean will be disturbed by nitrogen that returns to the ocean as NH_4^+ instead of NO_3^- .

Accordingly, reactions (S.14) and (S.15) are also considered to implicitly take place at (the ocean-side of) the SWI, neutralising the diffusive return fluxes of NH_4^+ and HS^- to the ocean, and the impact of these reactions on the alkalinity in the bottom ocean water accounted for:

- for ammonium re-oxidation (reaction S.5 or S.14), we have $\Delta\text{Alk}_T = -\Delta\text{TNO}_3 + \Delta\text{TNH}_3 = 2\Delta\text{TNH}_3$, since $\Delta\text{TNO}_3 = -\Delta\text{TNH}_3$ in those equations;
- for sulfide re-oxidation (reaction S.6 or S.15), we have $\Delta\text{Alk}_T = -2\Delta\text{TSO}_4 = 2\Delta\text{HS}^-$, since $\Delta\text{TSO}_4 = -\Delta\text{HS}^-$ in those equations.

Here we have called up the explicit conservative expression of alkalinity (Wolf-Gladrow et al., 2007) to link ΔAlk_T to the other variations. Let us then denote the diffusive return fluxes of NH_4^+ and HS^- to the ocean provided by MEDUSA by $J_{\text{NH}_4^+}$ and J_{HS^-} , supposed to be positive as they represent sources for the ocean. Accordingly, $\Delta\text{TNH}_3 = -J_{\text{NH}_4^+} < 0$ and $\Delta\text{HS}^- = -J_{\text{HS}^-} < 0$, and we find that the above reactions provide an alkalinity *sink* equal to $2 \times (J_{\text{NH}_4^+} + J_{\text{HS}^-})$ in the bottom ocean water.

References

- Archer, D., Lyle, M., Rodgers, K., and Froelich, P.: What Controls Opal Preservation in Tropical Deep-Sea Sediments?, *Paleoceanography*, 8, 7–21, <https://doi.org/10.1029/92PA02803>, 1993.
- Archer, D. E.: Modeling the Calcite Lysocline, *J. Geophys. Res.*, 96, 17 037–17 050, <https://doi.org/10.1029/91JC01812>, 1991.
- Arndt, S., Regnier, P., Godd eris, Y., and Donnadieu, Y.: GEOCLIM *reloaded* (v 1.0): a new coupled earth system model for past climate change, *Geosci. Model Dev.*, 4, 451–481, <https://doi.org/10.5194/gmd-4-451-2011>, 2011.
- Boudreau, B. P.: Asymptotic forms and solutions of the model for silica-opal diagenesis in bioturbated sediments, *J. Geophys. Res.*, 95, 7367–7379, <https://doi.org/10.1029/JC095iC05p07367>, 1990.
- Boudreau, B. P.: *Diagenetic Models and Their Implementation*, Springer-Verlag, Berlin (DE), 1997.
- Dickson, A. G., Sabine, C. L., and Christian, J. R., eds.: Guide to Best Practices for Ocean CO₂ Measurements, vol. 3 of *PICES Special Publication*, Carbon Dioxide Information and Analysis Center, Oak Ridge (TN), URL https://www.ncei.noaa.gov/access/ocean-carbon-acidification-data-system/oceans/Handbook_2007.html, 2007.
- Emerson, S.: Organic carbon preservation in marine sediments, in: *The Carbon Cycle and Atmospheric CO₂: Natural Variations Archean to Present*, edited by Sundquist, E. T. and Broecker, W. S., vol. 32 of *Geophys. Monogr. Ser.*, pp. 78–87, AGU, Washington (DC), <https://doi.org/10.1029/GM032p0078>, 1985.
- Hurd, D. C.: Interactions of biogenic opal, sediment and seawater in the Central Equatorial Pacific, *Geochim. Cosmochim. Acta*, 37, 2257–2282, [https://doi.org/10.1016/0016-7037\(73\)90103-8](https://doi.org/10.1016/0016-7037(73)90103-8), 1973.
- Jourabchi, P., Meile, C., Pasion, L. R., and Van Cappellen, P.: Quantitative interpretation of pore water O₂ and pH distributions in deep-sea sediments,

- Geochim. Cosmochim. Acta, 72, 1350–1364, <https://doi.org/10.1016/j.gca.2007.12.012>, 2008.
- Keir, R. S.: The dissolution kinetics of biogenic calcium carbonates in seawater, *Geochim. Cosmochim. Acta*, 44, 241–252, [https://doi.org/10.1016/0016-7037\(80\)90135-0](https://doi.org/10.1016/0016-7037(80)90135-0), 1980.
- Millero, F. J., Hubinger, S., Fernandez, M., and Garnett, S.: Oxidation of H₂S in seawater as a function of temperature, pH, and ionic strength, *Environ. Sci. Technol.*, 21, 439–443, <https://doi.org/10.1021/es00159a003>, 1987.
- Morse, J., Millero, F., Cornwell, J., and Rickard, D.: The chemistry of the hydrogen sulfide and iron sulfide systems in natural waters, *Earth Sci. Rev.*, 24, 1–42, [https://doi.org/10.1016/0012-8252\(87\)90046-8](https://doi.org/10.1016/0012-8252(87)90046-8), 1987.
- Munhoven, G.: Model of Early Diagenesis in the Upper Sediment with Adaptable complexity – MEDUSA (v. 2): a time-dependent biogeochemical sediment module for Earth system models, process analysis and teaching, *Geosci. Model Dev.*, 14, 3603–3631, <https://doi.org/10.5194/gmd-14-3603-2021>, 2021.
- Soetaert, K., Herman, P. M. J., and Middelburg, J. J.: A model of early diagenetic processes from the shelf to abyssal depths, *Geochim. Cosmochim. Acta*, 60, 1019–1040, [https://doi.org/10.1016/0016-7037\(96\)00013-0](https://doi.org/10.1016/0016-7037(96)00013-0), 1996.
- Thullner, M., Dale, A. W., and Regnier, P.: Global-scale quantification of mineralization pathways in marine sediments: A reaction-transport modeling approach, *Geochem., Geophys., Geosyst.*, 10, Q10012, <https://doi.org/10.1029/2009GC002484>, 2009.
- Van Cappellen, P. and Wang, Y.: Metal Cycling in Surface Sediments: Modeling the Interplay of Transport and Reaction, in: *Metal Contaminated Aquatic Sediments*, edited by Allen, H. E., chap. 2, pp. 21–64, Ann Arbor Press, <https://doi.org/10.1201/9780203747643-2>, 1995.
- Van Cappellen, P. and Wang, Y.: Cycling of Iron and Manganese in Surface Sediments: A General Theory for the Coupled Transport and Reaction of Carbon, Oxygen, Nitrogen, Sulfur, Iron, and Manganese, *Am. J. Sci.*, 296, 197–243, <https://doi.org/10.2475/ajs.296.3.197>, 1996.
- Wang, Y. and Van Cappellen, P.: A multicomponent reactive transport model of early diagenesis: Application to redox cycling in coastal marine sediments, *Geochim. Cosmochim. Acta*, 60, 2993–3014, [https://doi.org/10.1016/0016-7037\(96\)00140-8](https://doi.org/10.1016/0016-7037(96)00140-8), 1996.
- Wolf-Gladrow, D. A., Zeebe, R. E., Klaas, C., Körtzinger, A., and Dickson, A. G.: Total alkalinity: The explicit conservative expression and its application to biogeochemical processes, *Mar. Chem.*, 106, 287–300, <https://doi.org/10.1016/j.marchem.2007.01.006>, 2007.